

# Proceedings of the International Symposium on Enhanced Landfill Mining



**ELFM III**  
EURELCO

Third International  
Academic Symposium  
on Enhanced Landfill Mining



**FEBRUARY**  
8-10 • 2 • 2016

**LISBOA**  
**PORTUGAL**



## COPYRIGHTS

### TITLE

Proceedings of the International Symposium on Enhanced Landfill Mining

### EDITORS

Maria João Pereira, Maria Teresa Carvalho, Paula Falcão Neves

### EDITION

Instituto Superior Técnico  
Avenida Rovisco Pais  
1049-001 Lisboa

### ISBN

978-989-98342-4-8



## DISCLAIMER

Although all care is taken to ensure the integrity and quality of this publication and the information herein, no responsibility is assumed by the Publisher or the author for any damage to property or persons as a result of operation or use of this publication and/ or the information herein.

# Reuse of glass wastes from end-of-life fluorescent lamp in geopolymers for construction materials

Rui M. NOVAIS<sup>1</sup>, L.H. BURUBERRI<sup>1</sup>, G. ASCENSÃO<sup>1</sup>, M.P. SEABRA<sup>1</sup>, C. Dias-FERREIRA<sup>1</sup>, J.A. LABRINCHA<sup>1</sup>

<sup>1</sup> Department of Materials and Ceramic Engineering / CICECO – Aveiro Institute of Materials, University of Aveiro, Aveiro, Portugal

ruimnovais@ua.pt, leirehernando@ua.pt, guilhermeascensao@ua.pt, pseabra@ua.pt, cdf@ua.pt, jal@ua.pt

## Abstract

Nowadays the volume of generated wastes is reaching critical levels, which associated with the depletion of raw materials, shows that a paradigm shift is mandatory. The possibility of using waste materials as partial replacement of raw materials emerges as an opportunity to mitigate the environmental impact of wastes, while reducing the pressure exerted on the Earth's natural resources. In this work, a local and unexplored waste material coming from the recycling of end-of-life fluorescent lamps (glass wastes) was successfully incorporated in geopolymers production. Glass wastes were used, without any treatment, a source of amorphous silica to partially replace metakaolin.

## Introduction

End-of-life fluorescent lamps belong to the category of waste from electrical and electronic equipment (WEEE), and are one of the priority waste streams of EU policy. According to the latest data, approximately 1.1 thousand tonnes of fluorescent lamps were sold in Portugal in 2014<sup>0</sup>. Being a regulated waste stream, European countries have in place the source-separated collection of this waste. Collected lamps are contaminated with dangerous substances such as mercury, or other lamp components (e.g. plastic, metal) which hinders their re-use or recycling. Hence, this waste is forwarded to recycling facilities where it is treated and sorted into several streams: ferrous metals (0.6%), non-ferrous metals (1.4%), glass (93.9%) and others (4.1%)<sup>0</sup>. Even though the recovery of valuable materials contained in the lamps is already in place, it will take more effort to develop the necessary processes that will promote the

transformation of recovered materials into new products. There is a fluorescent lamp recycling facility in Portugal producing ~400 t/year of contaminated glass waste (GW)<sup>0</sup>. This accumulated pre-treated GW is an unexplored secondary raw material.

Geopolymers are inorganic aluminosilicate polymers synthesized by alkali activation of Si- and Al-rich materials at near ambient temperatures<sup>0</sup>. This technology has attracted increasing attention since it is considered as a viable solution for reusing industrial wastes, providing a cost-effective and sustainable approach for hazardous residues<sup>0,0</sup>. Nevertheless, geopolymerization is a rather complex process, in particular when using waste materials. The development of geopolymers from wastes is a challenge, since the materials are less reactive and less soluble than the commonly used raw materials, and have elements that can be detrimental to the geopolymerization process. Yet, waste based-geopolymers can be optimized and tailored to a desired application.

In this work, unexplored glass waste was initially characterized to assess its potential as an aluminosilicate source in geopolymers production. Hence, the substitution of metakaolin (MK), the benchmark raw material in geopolymers production, by these GW was investigated. The influence of solids-to-liquid (S/L) ratio, which corresponds to the aluminosilicate-to-activator solution ratio, and curing time on the microstructure, physical and mechanical properties of the produced geopolymers was studied.

## **Experimental**

### **Materials**

Geopolymers were prepared using a mixture of 3/4 MK and 1/4 GW as binders. The MK was purchased under the name of Argical™ M1200S from Univar®, while GW was supplied by a Portuguese lamp recycling company “Ambicare S.A.” located in Setúbal. The GW comes from the recycling of fluorescent lamps that have been previously treated for recovery of mercury and rare earth elements; nevertheless it is still severely contaminated with metal, plastic and other residues. The GW was crushed in a mortar and sieved through a 75 µm mesh prior to mixing.

For the alkaline activation, a mixture of hydrated sodium silicate (Chem-Lab, Belgium; 8.5 wt.% Na<sub>2</sub>O, 28.5 wt.% SiO<sub>2</sub> and 63 wt.% H<sub>2</sub>O) and NaOH (reagent grade, 97%, Sigma Aldrich) was used. The NaOH solution was prepared by dissolution of 20-40 mesh sodium hydroxide beads in distilled water.

### **Geopolymers preparation**

To evaluate the influence of the raw materials mixing ratio, three different formulations were prepared containing distinct S/L ratios, namely 0.63, 0.71 and 0.80. The SiO<sub>2</sub>/Al<sub>2</sub>O<sub>3</sub> molar ratio for these formulations was, respectively, 3.8, 3.7 and 3.6.

The mixing of the blends was carried out by a mechanical process which involves: i) homogenization of sodium silicate and NaOH solution (12M) at 60 rpm for 5 min, and ii) mixture at the same speed of the alkaline solution with a previously homogenised mix of GW and MK for 10 min.

Then, the slurry was transferred to plastic moulds and sealed with a plastic film. The samples were cured in controlled conditions (40 °C and 65% relative humidity) using a climatic chamber for 24 hours. Afterwards, the specimens were demoulded and kept sealed in the same curing conditions until the 7<sup>th</sup> curing day. Then the samples were left at ambient conditions until the 28<sup>th</sup> curing day.

### **Material characterization**

Scanning electron microscopy (SEM - Hitachi S4100 - equipped with energy dispersion spectroscopy, EDS – Rontec) was used to characterize the MK, the GW and to investigate the microstructure of the geopolymers.

The mineralogical compositions of MK, GW and geopolymer specimens cured for 28 days were assessed by X-ray powder diffraction (XRD). The XRD was conducted on a Rigaku Geigerflex D/max-Series instrument (Cu K $\alpha$  radiation, 10–80°, 0.02° 2 $\theta$  step-scan and 10 s/step), and phase identification by X'Pert HighScore Plus software.

The chemical composition of GW and MK was obtained by using X-ray fluorescence (Philips X'Pert PRO MPD spectrometer). The loss on ignition (LOI) at 1000°C was also determined. Particle size distribution was determined by laser diffraction (Coulter LS230 analyzer). The determination was performed by a laser diffraction technique (Fraunhofer method) for particles with a particle size from 0.4  $\mu\text{m}$  to 200  $\mu\text{m}$  and simultaneously by PIDS (Polarization Intensity Differential Scattering) for smaller particles (between 0.4  $\mu\text{m}$  and 0.04  $\mu\text{m}$ ).

The compressive strength of geopolymers with distinct curing times was determined using a Universal Testing Machine (Shimadzu model AG-25 TA) running at a displacement rate of 0.5 mm min<sup>-1</sup>. Three cylindrical samples of each formulation (22 mm diameter and 48 mm length) were tested and the average data reported. Specimen's surfaces were polished to become flat and parallel.

The BET specific surface areas of the MK and GW were measured by N<sub>2</sub> adsorption using a 5-point BET method. Measurements were conducted on a Micromeritics Gemini 2380 analyzer with ca. 250 mg of each sample. Standard pretreatment conditions were 105 °C and vacuum for 12 h.

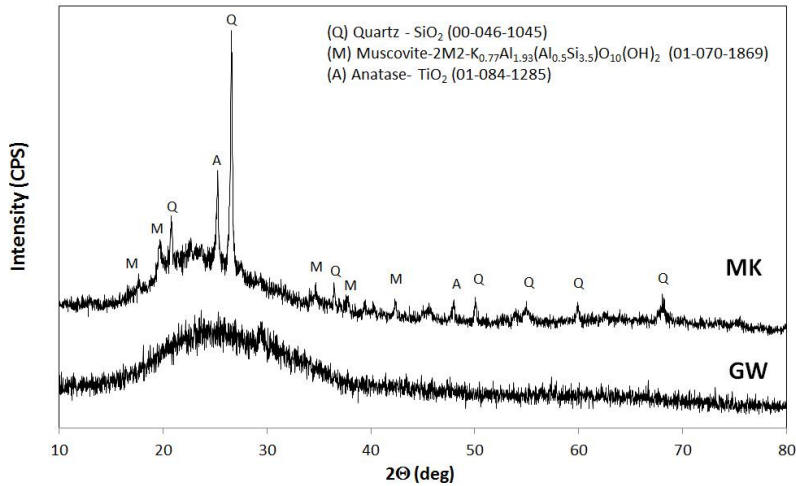
## Results and discussion

### Raw materials characterization

The chemical composition of GW, shown in Table 1, indicates a clear dominance of SiO<sub>2</sub>, Na<sub>2</sub>O, CaO, MgO and Al<sub>2</sub>O<sub>3</sub> being the other significant oxides. In fact, this is the expected composition for a common glass. The XRD pattern of GW demonstrates the highly amorphous nature of this material (see Fig. 1), confirmed by the absence of crystalline peaks. The expected high content of reactive silica of the GW, one of the most important factors in geopolymer formation<sup>0</sup>, indicates that it can be used as a source of silica on the preparation of geopolymers. For the MK, the XRD pattern shows a pronounced reflection between 20-30° which was attributed to the amorphous silica and alumina compounds. Nonetheless, a few crystalline peaks were also detected such as quartz, muscovite and anatase. Similar crystalline phases have been reported for MK previously<sup>0,0</sup>.

**Table 1:** Chemical composition of metakaolin (MK) and glass wastes (GW).

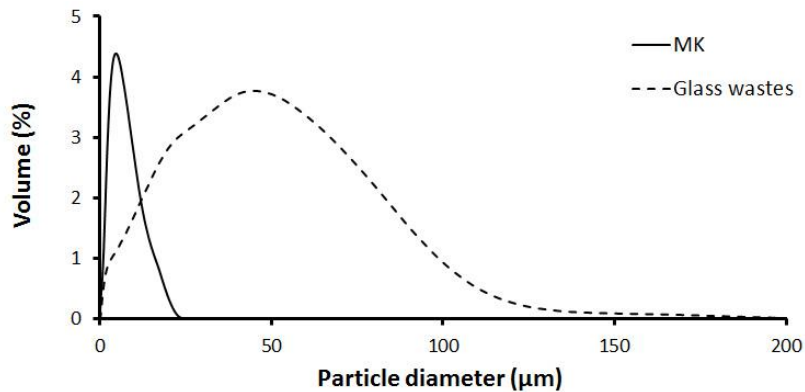
Oxides (wt.%)	MK	GW
SiO <sub>2</sub>	54.40	70.57
TiO <sub>2</sub>	1.55	0.05
Al <sub>2</sub> O <sub>3</sub>	39.40	2.48
Fe <sub>2</sub> O <sub>3</sub>	1.75	0.28
MgO	0.14	3.05
CaO	0.10	5.59
MnO	0.01	0.01
Na <sub>2</sub> O	-	14.49
K <sub>2</sub> O	1.03	1.35
SO <sub>3</sub>	-	0.19
P <sub>2</sub> O <sub>5</sub>	0.06	0.06
LOI	2.66	0.95



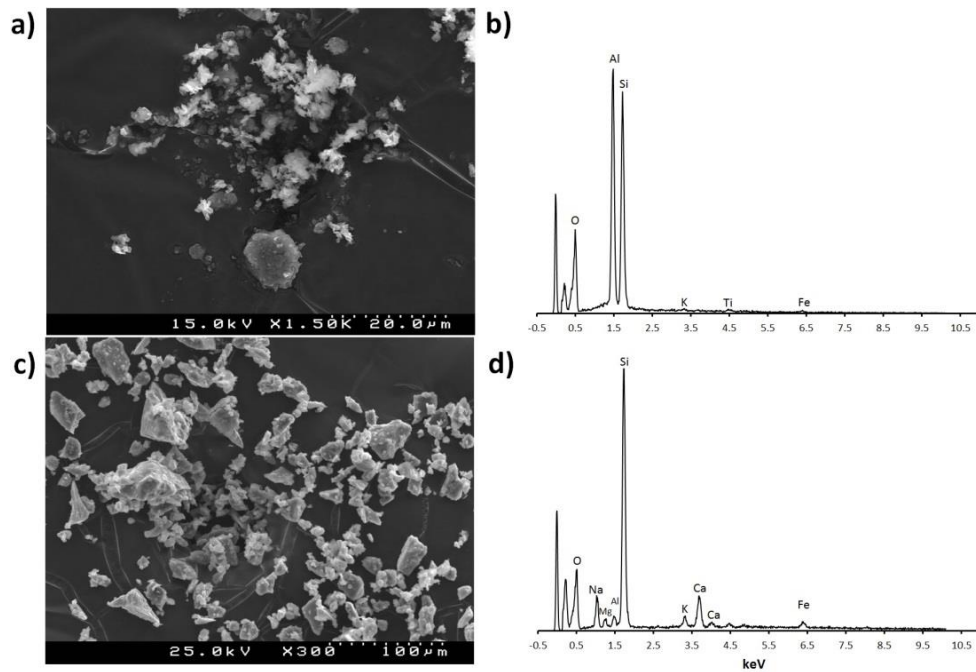
**Figure 1:** XRD patterns of fluorescent lamp glass wastes (GW) and metakaolin (MK).

Fig. 2 presents the particle size distribution for the GW and the MK. As observed, GW is composed by particles of larger size. Mean particle sizes of 31  $\mu\text{m}$  and 5  $\mu\text{m}$  were estimated for the GW and MK, respectively. In agreement, the specific surface area of the MK ( $26.15 \text{ m}^2/\text{g}$ ) is much higher than that of the GW ( $3.92 \text{ m}^2/\text{g}$ ). The particle size is known to strongly affect the material's reactivity<sup>0</sup>, and therefore the strength development<sup>0</sup>. Higher reactivity leads to faster dissolution of the raw materials, and improves the geopolymerization rate.

The differences in the particle size of the two materials are also illustrated by the SEM micrographs presented in Fig. 3. Fig 3c shows the irregular shape of the GW particles, while the EDS spectrum (Fig. 3d) reveals the presence of Si, Al, Na, Ca, Mg, K and Fe. The elements detected are in agreement with the chemical composition of the GW (see table 1). As expected, the EDS spectrum of the MK shows the presence of Al, Si, K, Ti and Fe (Fig. 3b).



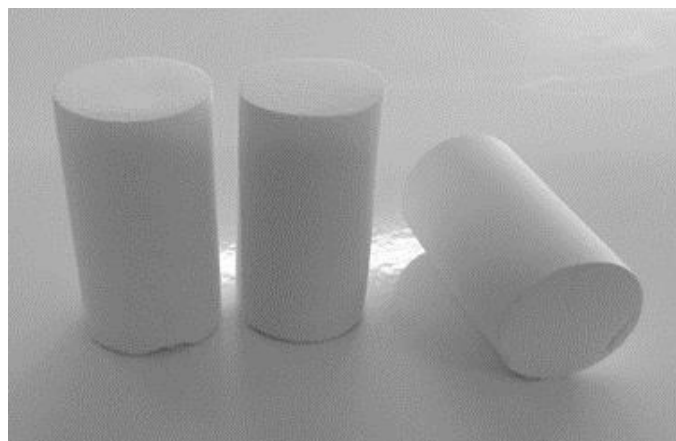
**Figure 2:** Particle size distribution of metakaolin and fluorescent lamp glass wastes.



**Figure 3:** SEM micrographs and EDS spectrum of metakaolin (a and b) and fluorescent lamp glass wastes (c and d).

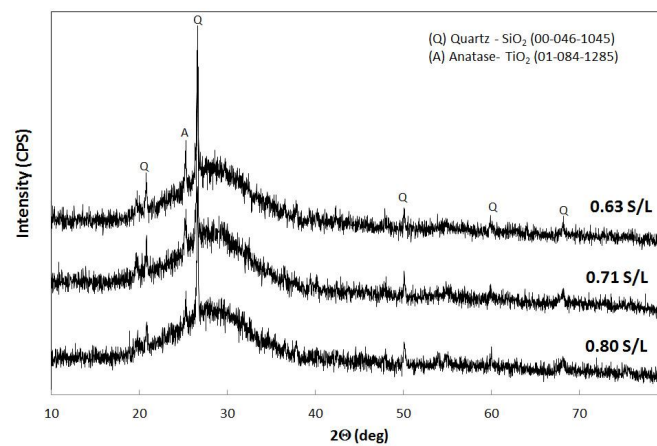
### Geopolymer characterization

Fig. 4 presents typical images of the GW-geopolymers, demonstrating that these unexplored wastes can be successfully incorporated in geopolymers.



**Figure 4:** Geopolymer cylindrical specimens (20 mm diameter and 40 mm length) obtained by addition of fluorescent lamp glass wastes.

The XRD patterns of geopolymers (cured for 28 days) prepared with distinct S/L ratio are shown in Fig. 5. A broad hump between 20-40° 2θ was observed in all patterns, which indicates the occurrence of geopolymerization reactions. Additionally, the centre of the hump shifts to the right towards higher 2θ values in comparison with that observed in the raw materials, providing evidence of the formation of new amorphous phases<sup>0</sup>. The geopolymerization reaction is expected to give rise to an amorphous aluminosilicate gel, and indeed, the SEM micrograph in Fig. 6 reveals the presence of such gel, mainly composed of Si, Al and Na. The gel was observed in all compositions (not shown here for the sake of brevity).



**Figure 5:** XRD patterns of fluorescent lamp glass waste-geopolymers produced with different solids-to-liquid ratio.

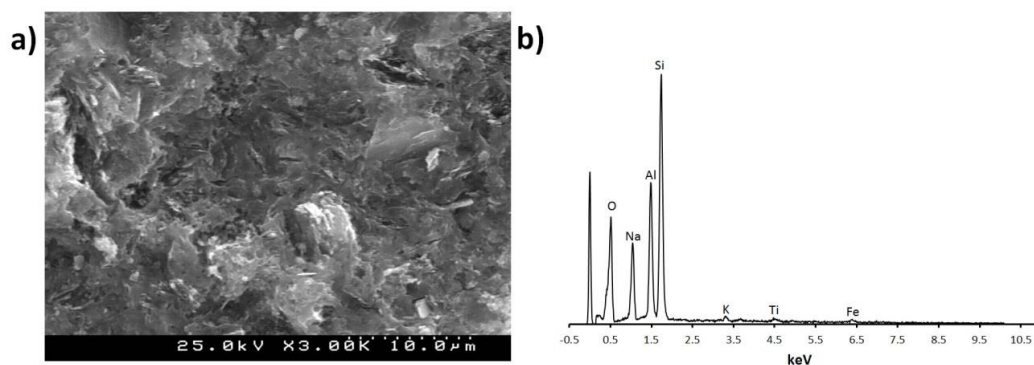


**Figure 6:** a) SEM micrograph and b) EDS spectrum of fluorescent lamp glass waste-geopolymer produced with a solids-to-liquid ratio of 0.71.

Fig. 7 presents SEM micrographs of the GW-containing geopolymers produced with different S/L ratios. Clearly, the microstructural development of the prepared geopolymers is strongly affected by this ratio, namely the porosity (number and area of pores): larger pores are observed when the ratio is 0.63, and a high number of smaller pores are present when the ratio is 0.80. These round pores are possibly associated with entrapped air during mixing<sup>0</sup>. In fact, the workability of the formulation prepared with 0.80 S/L ratio was significantly affected (the mix is stiffer), which hindered the casting of the slurry in the plastic moulds, thus offering an opportunity for air entraining.

The number of unreacted glass particles (identified by white arrows) is also affected by the S/L ratio. All formulations present unreacted glass particles, yet when the ratio is above 0.71, their number increases greatly, suggesting a lower degree of the geopolymeric reaction. These unreacted glass particles, and the number and area of pores, are expected to affect the mechanical resistance of the geopolymers. Indeed, Fig. 8 shows that the highest compressive strength was achieved with an S/L of 0.71. This sample also presented lower porosity, and a smaller number of unreacted glass particles. Provis *et al.*<sup>0</sup> observed that geopolymers prepared with very high S/L ratios generally do not show high strength, while Zuhua *et al.*<sup>0</sup> stated that low S/L ratios accelerate the dissolution of raw materials hinder the polycondensation process at high NaOH concentration, which is in agreement with our results. The influence of S/L ratio on the mechanical resistance of geopolymers was also reported by other authors<sup>15,16</sup>.

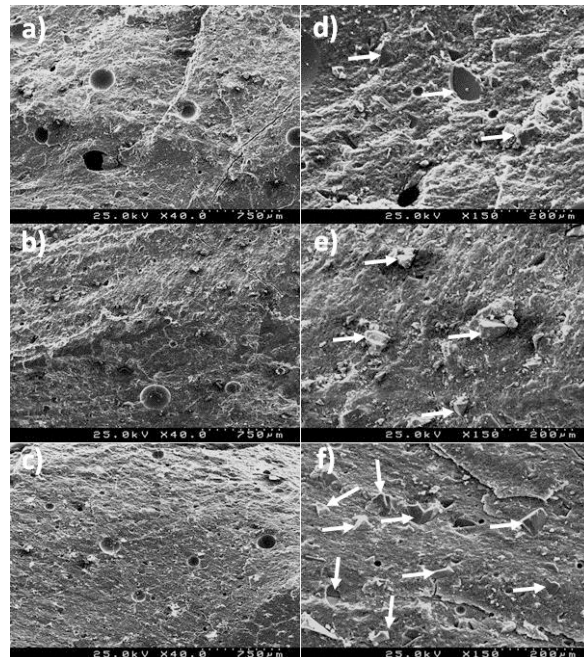


**Figure 7:** SEM characterization of GW-containing geopolymers produced with different solids-to-liquid ratio: 0.63 (a and d), 0.71 (b and e) and 0.80 (c and f). The white arrows identify non-reactive glass waste particles.

The data presented in Fig. 8 also show the expected increase in the compressive strength with ageing for all compositions studied.

The maximum compressive strength attained for the GW-geopolymers (24.6 MPa) demonstrates the potential of this novel material for structural applications.

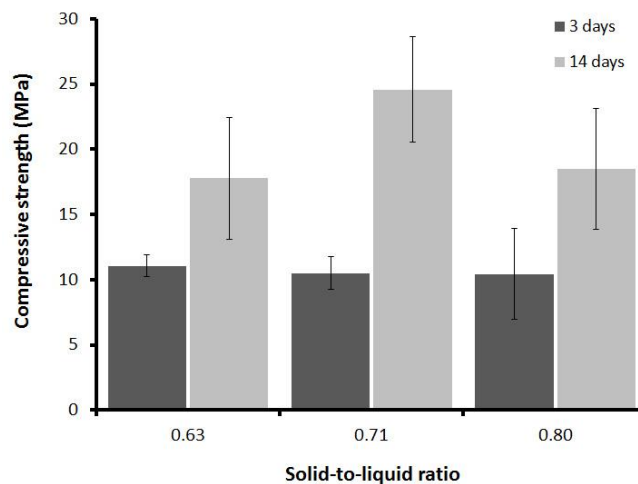


**Figure 8:** Influence of curing time on the compressive strength of GW-containing geopolymers produced with different solids-to-liquid ratios.

## Conclusions

In the present work, glass waste from end-of-life fluorescent lamps was successfully incorporated in geopolymers. These unexplored glass wastes were used to partially replace metakaolin, with obvious advantages both from environmental and economic viewpoints.

The solids-to-liquid ratio and the curing time were found to significantly affect the properties of the produced GW-containing geopolymers. The best results were achieved with an S/L of 0.71, while higher and lower S/L ratios hindered the geopolymerization reaction. GW-geopolymers showing compressive strength of 24.6 MPa were fabricated.

This work demonstrates the feasibility of producing waste based-geopolymers with potential as construction materials, using a simple and eco-friendly approach.

Furthermore, the incorporation of local and unexplored residue (fluorescent lamp waste glass) is a positive contribute towards sustainable construction.

## Acknowledgements

Thank you to Dr RC Pullar for assistance with the English of this article.

## References

1. Annual Market Report (2014) from the National Association for the Registration of Electrical and Electronic Equipment (Portugal). Available from: <https://www.anreee.pt/>.
2. M. Crowe, A. Elser, B. Gopfert, L. Mertins, T. Meyer, J. Schmid, A. Spillner, R. Strobel, "Waste from electrical and electronic equipment (WEEE) - Quantities, dangerous substances and treatment methods", *European Environment Agency*, January (2003).
3. K. Komnitsas, D. Zaharaki, "Geopolymerization: a review and prospects for the minerals industry", *Mineral Engineering*, 20, 1261-1277 (2007).
4. W. Hajjaji, S. Andrejkovičová, C. Zanelli, M. Alshaaer, M. Dondi, J.A. Labrincha, F. Rocha, "Composition and technological properties of geopolymers based on metakaolin and red mud", *Materials and Design*, 52, 648-654 (2013).
5. J. Zhang, J.L. Provis, D. Feng, J.S.J. van Deventer, "Geopolymers for immobilization of  $\text{Cr}^{6+}$ ,  $\text{Cd}^{2+}$ , and  $\text{Pb}^{2+}$ ", *Journal of Hazardous Materials*, 157, 587-598 (2008).
6. M. Torres-Carrasco, F. Puertas, "Waste glass in the geopolymer preparation. Mechanical and microstructural characterization", *Journal of Cleaner Production*, 90, 397-408 (2015).
7. A. Cwirzen, J.L. Provis, V. Penttala, K. Habermehl-Cwirzen, "The effect of limestone on sodium hydroxide-activated metakaolin-based geopolymers", *Construction and Building Materials*, 66, 53-62 (2014).
8. A. Autef, E. Joussein, G. Gasgnier, S. Pronier, I. Sobrados, J. Sanz, S. Rossignol, "Role of metakaolin dehydroxilation in geopolymer synthesis", *Powder Technology*, 250, 33-39 (2013).
9. A. Nazari, A. Bagheri, S. Riahi, "Properties of geopolymer with seeded fly ash and rice husk bark ash", *Materials Science and Engineering A*, 528, 7395-7401 (2011).
10. J. He, J. Zhang, Y. Yu, G. Zhang, "The strength and microstructure of two geopolymers derived from metakaolin and red mud-fly ash admixture: a comparative study", *Construction and Building Materials*, 30, 80-91 (2012).
11. M. Zhang, T. El-Korchi, G. Zhang, J. Liang, M. Tao, "Synthesis factors affecting mechanical properties, microstructure, and chemical composition of red mud-fly ash based geopolymers", *Fuel*, 134, 315-325 (2014).
12. A.I. Badanoiu, T.H.A. Al Saadi, S. Stoleriu, G. Voicu, "Preparation and characterization of foamed geopolymers from waste glass and red mud", *Construction and Building Materials*, 84, 284-293 (2015).

13. J.L. Provis, C.Z. Yong, P. Duxson, J.S.J. van Deventer, "Correlating mechanical and thermal properties of sodium silicate-fly ash geopolymers", *Colloids and Surfaces A: Physicochem. Eng. Aspects*, 336, 57–63 (2009).
14. Z. Zuhua, Y. Xiao, Z. Huajun, C. Yue, "Role of water in the synthesis of calcinated kaolin-based geopolymers", *Applied Clay Science*, 43, 218-223 (2009).
15. C. Y. Heah, H. Kamarudin, A.M.M. Al Bakri, M. Bnhussain, M. Luqman, I.K. Nizar, C.M. Ruzaidi, Y.M. Liew, "Study on solids-to-liquid and alkaline activator ratios on kaolin-based geopolymers", *Construction and Building Materials*, 35, 912-922 (2012).
16. Y.M. Liew, H. Kamarudin, A.M.M. Al Bakri, M. Bnhussain, M. Luqman, I.K. Nizar, C.M. Ruzaidi, C. Y. Heah, "Optimization of solids-to-liquid and alkali activator ratios of calcinated kaolin geopolymeric powder", *Construction and Building Materials*, 37, 440-451